UNIVERSITY OF BIRMINGHAM

Bandwidth enhancement of circularly polarised slot global navigation satellite systems antenna using an integrated filter-antenna approach

Aly, Mostafa G.; Wang, Yi

Document Version
Publisher's PDF, also known as Version of record

[Link to publication on Research at Birmingham portal](#)

IET Microwaves, Antennas & Propagation

The Institution of Engineering and Technology WILEY

ORIGINAL RESEARCH PAPER

Bandwidth enhancement of circularly polarised slot global navigation satellite systems antenna using an integrated filter-antenna approach

Mostafa G. Aly[1] | Yi Wang[2]

[1]Faculty of Engineering and Science, University of Greenwich, Kent, UK

[2]Department of Electronic Electrical and Systems Engineering, University of Birmingham, Birmingham, UK

Correspondence

Mostafa G. Aly, Faculty of Engineering and Science, University of Greenwich, Kent, ME4 4TB, UK.
Email: M.G.Aly@greenwich.ac.uk

Abstract:

A technique to enhance the bandwidth of a circularly polarised antenna using the filter-antenna design approach is presented. The design relies on adding a resonator coupled to the radiation element—an L-shaped slot antenna in the case of global navigation satellite systems. This change in the feeding structure broadens both the impedance and the axial ratio (AR) bandwidths and allows more design flexibility. Compared with a reference L-shaped slot antenna with a conventional feed, the proposed antenna design achieves a doubling of the impedance matching bandwidth from 19% to 41% over the frequency range from 1.2 to 1.81 GHz and a wider AR bandwidth from 35% to 44.5% in the range from 1.17 to 1.84 GHz. The AR bandwidth covers the entire impedance bandwidth. The effect of a metal reflector on antenna performance is also investigated and discussed.

1 | INTRODUCTION

Circularly polarised (CP) antennas possess important features for a wide range of applications including radio-frequency identifications, radars, and satellites such as global navigation satellite systems (GNSSs). The key advantages of a CP antenna are its immunity to restricted orientation [1] and its ability to reject multipath signals, therefore enhancing the receiving antenna's polarisation efficiency [2]. A wide range of CP antennas have been reported to have a wide axial ratio bandwidth (ARBW) to cope with the high channel capacity demanded by modern wireless systems. For example, this can be realised using slot antennas with L-shaped feedlines [3], vertical L-shaped ground planes [4], cross dipoles in the presence of phase delay lines [5–7] or asymmetric T-strips fed via coplanar waveguides [8]. Monopole antennas are also a common approach to achieve wideband CP antennas [9–11]. While using dual-feed or multiple substrates can usually enhance bandwidth [12–14], it is at the expense of more complicated fabrications, and therefore, higher cost. Single-feed slot antennas are simple to fabricate and have a low profile, but usually with a narrow bandwidth and low gain values for being bidirectional. Metal reflectors are traditionally placed at a quarter wavelength to increase directivity [8, 13, 15] at the expense of reduced bandwidth.

An integrated filter-antenna concept is adopted here to increase the bandwidth of a single-feed CP antenna by introducing electromagnetic (EM) coupling. The concept has received renewed interest in recent years and mostly for linearly polarised antennas [16, 17]. An increasing number of CP antennas with integrated filters are also being reported. Embedded filters in the antenna feedline are reported in [18, 19], whereas in [20, 21, 22], the resonant radiation element was treated as the last resonator in a filter.

This work is based on the bidirectional L-shaped slot antenna reported in [15]. With a low circuit complexity in mind, an edge-coupled resonator was used to feed the radiation element via EM coupling. The antenna element acts as the second resonator in a second-order filtering circuit. This results in a second-order filtering CP antenna, aiming to cover the entire GNSS operating band from 1.16 to 1.6 GHz.

The integrated design is described in Section 2. The antenna is designed using the Computer Simulation Technology (CST) Microwave Studio simulator. Parametric studies are elaborated on in Section 3. Measurement results are discussed in Section 4. The investigation of the metal reflector is deliberated in Section 5. Section 6 concludes the paper.

2 | FILTERING CIRCULARLY POLARISED ANTENNA DESIGN

The CP slot antenna first reported in [15] is chosen as a baseline design for comparison. This reference design is modified to operate at the GNSS band with a centre frequency f_0 of 1.5 GHz. The resulting reference design is a single-feed CP antenna with a C-shaped microstrip line to excite the L-shaped slot, as shown in Figure 1. The vertical and horizontal sections of the slots support orthogonal electric fields. The C-shaped feedline excites the two sections in sequence. With optimised dimensions of the feedline, 90° phase shift can be achieved in the excitations to generate circular polarisation. The antenna was built on a single substrate of Rogers RO4003C with a dielectric constant of 3.55 and 0.813 mm thick. The simulated results of such a design are presented in Figure 2. It recorded a return loss (over 10 dB) bandwidth (RLBW) from 1.4 to 1.72 GHz (19%) and an ARBW from 1.35 to 1.92 GHz (35%) for an axial ratio (AR) under 3 dB.

The new proposed filtering CP antenna is detailed in Figure 3. The microstrip line from the input port is edge-coupled to a U-shaped resonator on one side of the substrate, which excites the L-shaped slot on the other side. Like the reference design in principle but with a resonant structure, the vertical and horizontal sections of the resonator excite the vertical and horizontal parts of the
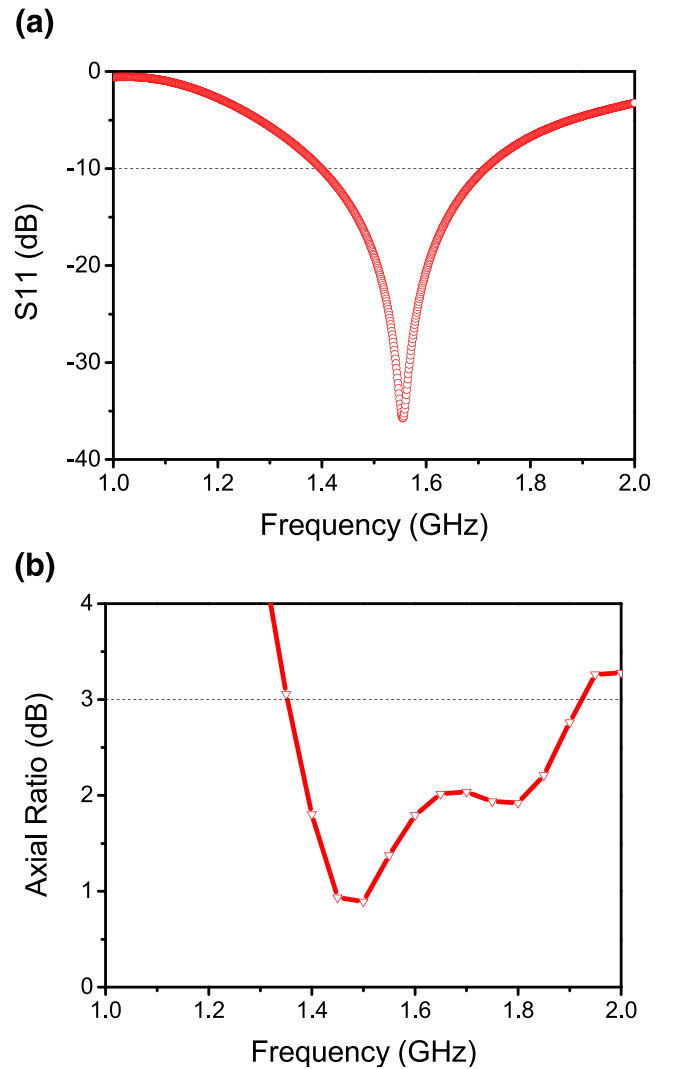

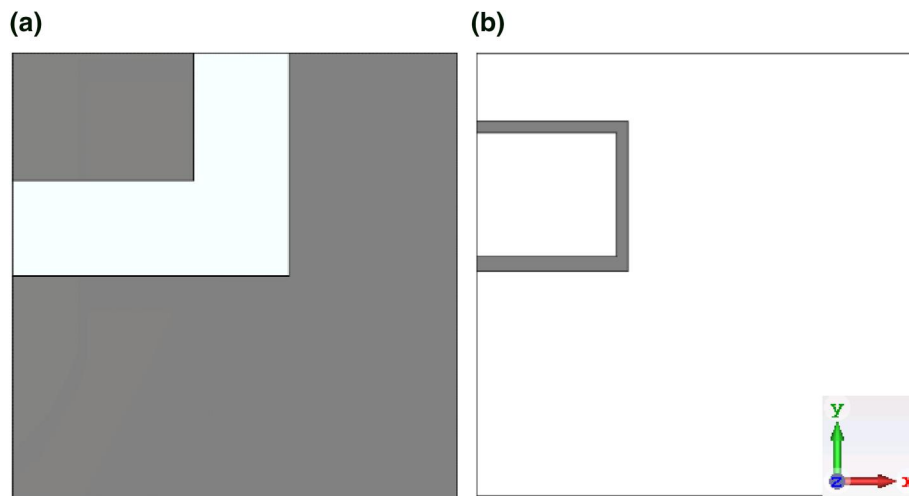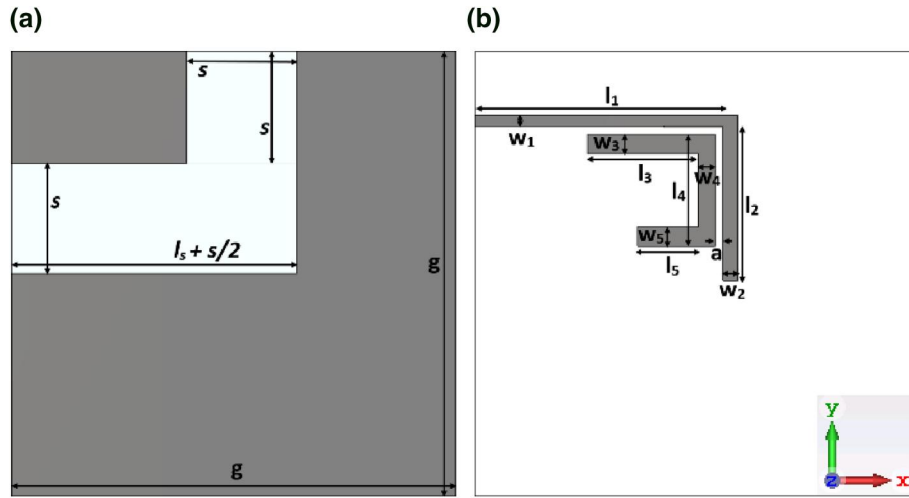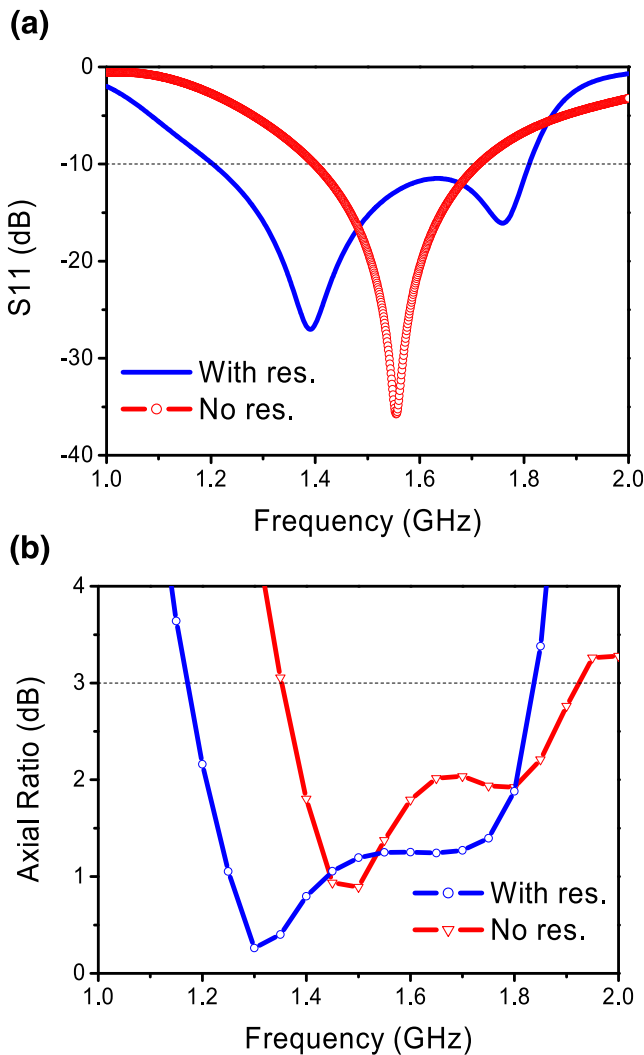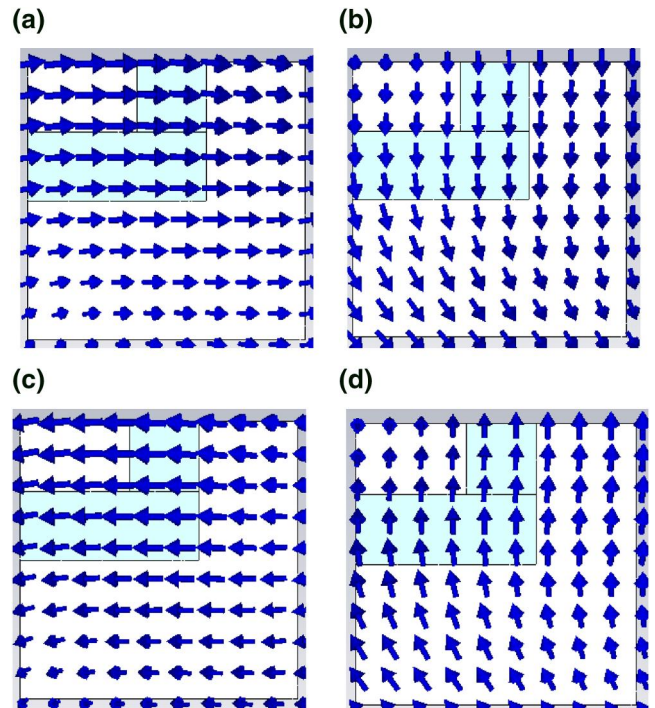**FIGURE 2** Simulated reference circularly polarised antenna (a) S_{11} (b) Axial ratio

FIGURE 1 The reference circularly polarised antenna with a C-shaped feedline [15] (a) Front (b) Back

FIGURE 3 The proposed filtering circularly polarised antenna with a resonator feed (a) Front (b) Back $g = 80$, $s = 19.8$, ls = 41.5, $l_1 = 44.6$, $w_1 = 1.85$, $l_2 = 27.65$, $w_2 = 2.65$, $l_3 = 20$, $w_3 = w_5 = 3.4$, $l_4 = 20$, $w_4 = 3$, $l_5 = 11$, a = 1.4 (unit: mm)

FIGURE 5 Simulated E-field distribution at 50 mm above the surface at 1.5 GHz for different phase angles: (a) $\omega t = 0°$ (b) $\omega t = 90°$ (c) $\omega t = 180°$ (d) $\omega t = 270°$

FIGURE 4 Simulated circularly polarised slot antenna with and without resonator feed: (a) S11 (b) Axial ratio

slots. The required quadrature phase is achieved by the phase difference between the vertical and horizontal feeding sections. An important feature here is that the coupling between the microstrip line and the resonator, and between the resonator and the slot, controls the antenna bandwidth. It is also worth noting that having different horizontal lengths for the resonator helps balance the magnitudes of the EM fields for the horizontal and vertical polarisations.
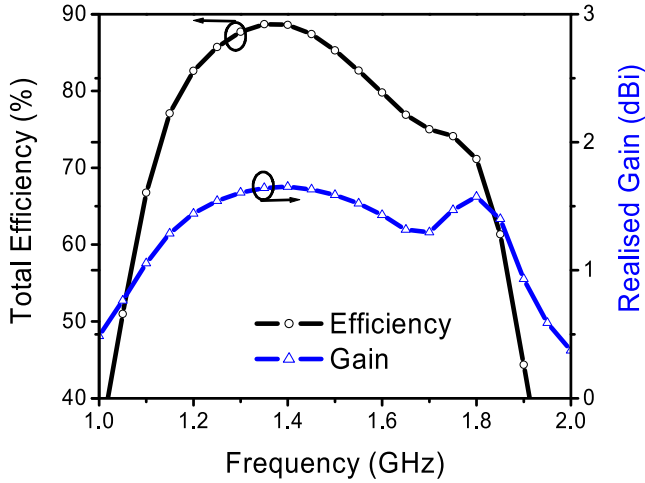
FIGURE 6 Simulated total efficiency and realised gain
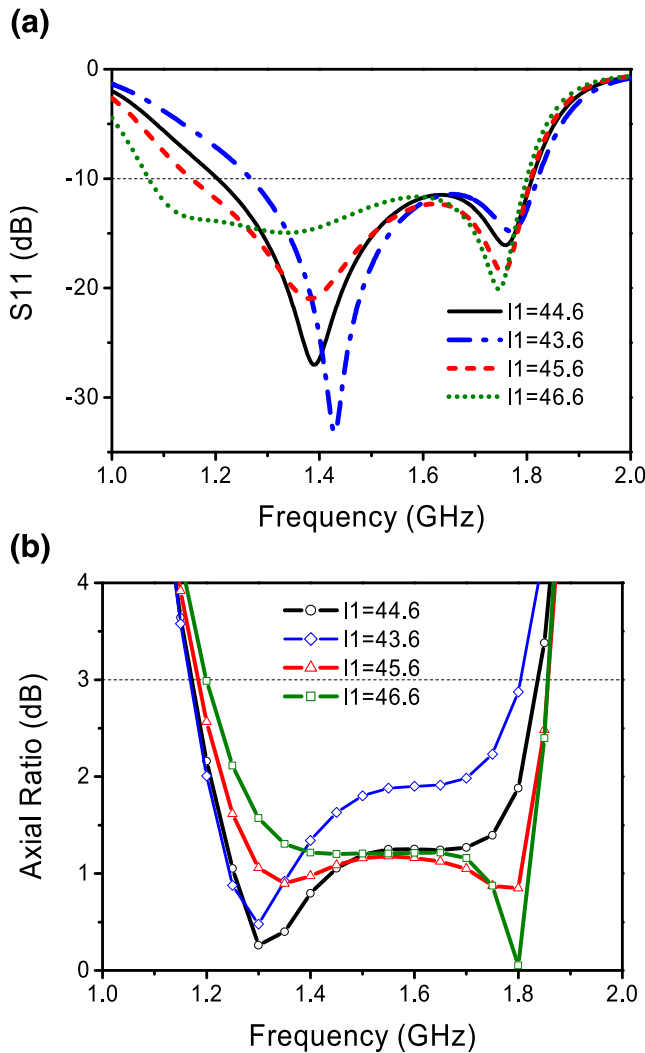
FIGURE 7 Effect of feedline length (L_1) on (a) S_{11} (b) Axial ratio
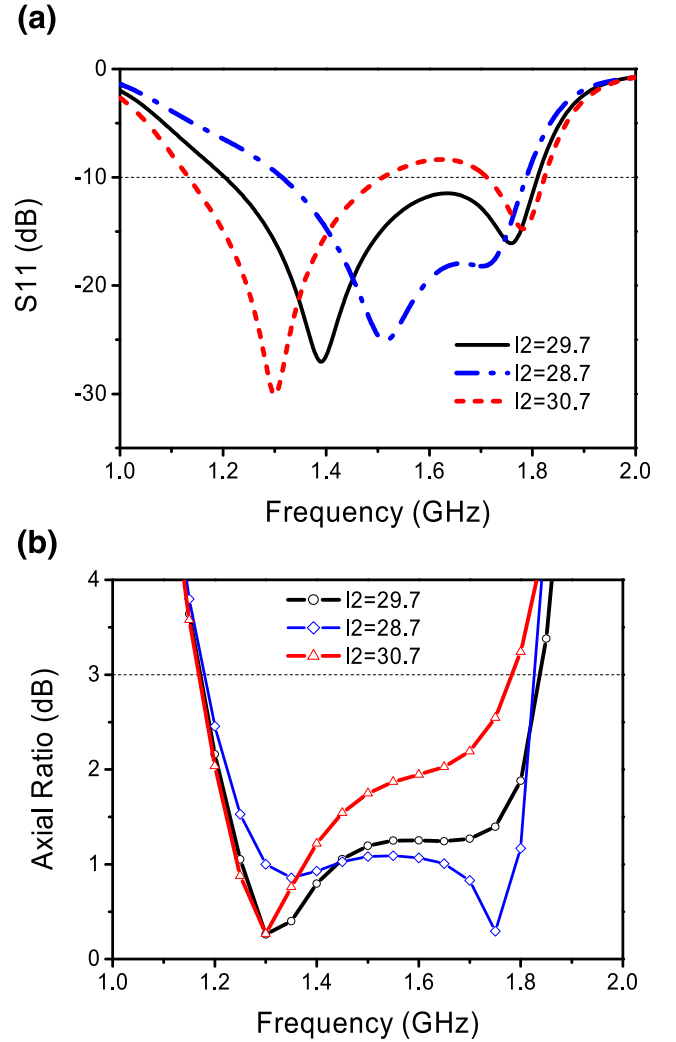
FIGURE 8 Effect of coupling line length (L_2) on (a) S_{11} (b) Axial ratio

The proposed antenna was designed using the same substrate with an overall size of 80×80 mm. The effective length of the L-shaped slot is roughly a half-guided wavelength ($\lambda_g/2$) of 54 mm at 1.5 GHz and deduced from the following equation [23]:

$$L_{eff} = \frac{c}{2f_0\sqrt{\epsilon_{eff}}} \tag{1}$$

where c is the speed of light, and ε_{eff} is the effective dielectric constant. The lengths of the vertical and horizontal arms of the L-shaped slot were optimised to realise the CP operation.

Figure 4 compares the performance between the conventional C-shaped feed and the proposed resonator feed in terms of S_{11} and AR responses. For the proposed integrated filter-antenna design, two reflection dips (matching points) appear in the impedance bandwidth because of the coupling between the resonator and the L-shaped slot.

The RLBW is doubled to 41% (1.2 to 1.81 GHz), with a 3–dB ARBW from 1.17 to 1.84 GHz (44.5%). The RLBW is entirely within the ARBW. This feature has rarely been reported in the literature before for the GNSS band. In [14], this was accomplished covering the ISM band.

To illustrate the CP operating mode of the antenna, the simulated electric-field distribution at 50 mm above the substrate is shown in Figure 5 for the centre frequency of 1.5 GHz. The polarisation rotation can be seen as a right-hand CP (RHCP) operation.

The proposed slot antenna has both forward and backward radiation (bidirectional), and thus, it has a low maximum gain. The simulated total efficiency is 82% on average over the targeted band, while the realised gain is 1.66 dBi on average, as shown in Figure 6. In Section 5, a metal reflector will be introduced to increase antenna directivity.

The coupling between the added resonator and the radiating slot is responsible for increasing the antenna bandwidth. The coupled-resonator filter design approach [24] was adopted in shaping the S_{11} response to create the two reflection zeros.

For the targeted fractional bandwidth (*FBW*) of 41% and return loss (RL) of 10 dB in a second-order filtering circuit, the g-element values were $g_0 = 0.6986$ and $g_1 = 1$. These values are translated to a coupling coefficient (*M*) and an external quality factor (Q_{ex}) using (2) and (3), resulting in values of 0.49 and 1.7, respectively:

$$M_{i,i+1} = \frac{FBW}{\sqrt{g_i \cdot g_{i+1}}} \quad (2)$$

$$Q_{ex} = \frac{g_i \cdot g_{i+1}}{FBW} \quad (3)$$

These obtained values are then used in the initial dimensioning of the circuit layout. It should be noted that the initial dimensions provide only a starting point for the optimisation. The resonant characteristics of the radiating slot are very different from the microstrip line resonator in terms of quality factor. For this reason, the dimensions extracted from *M* and

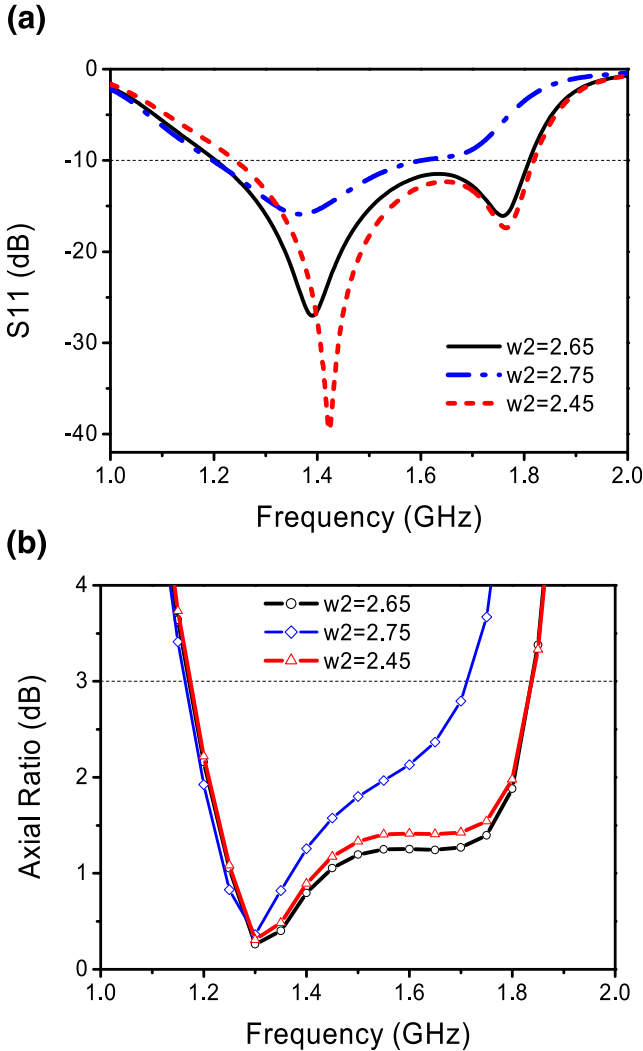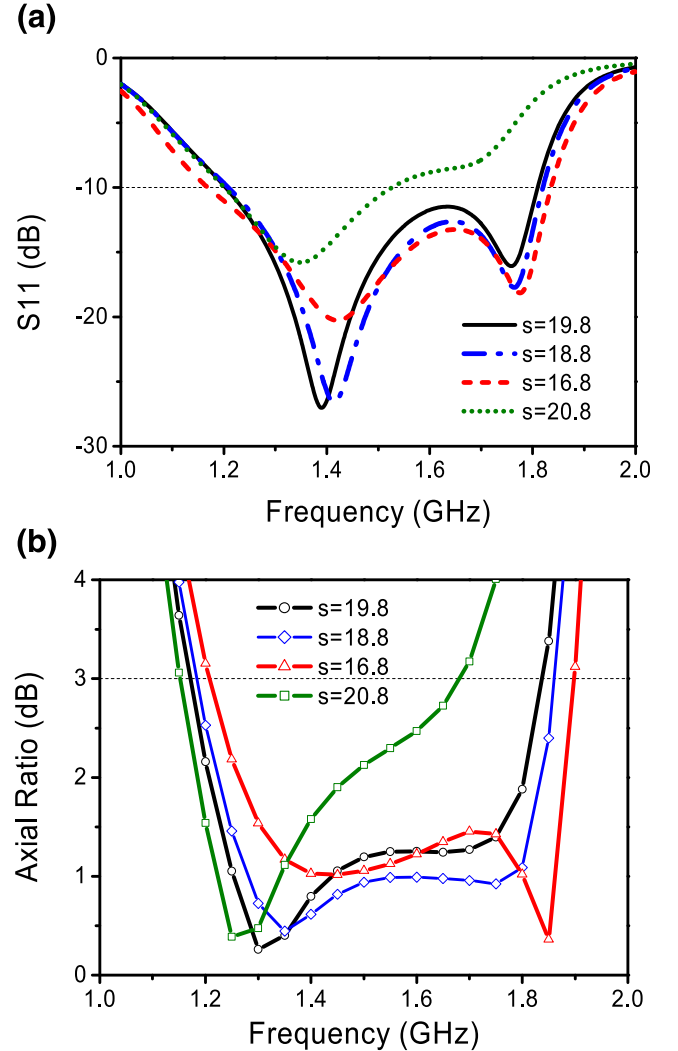**FIGURE 9** Effect of coupling line width (w_2) on (a) S11 (b) Axial ratio

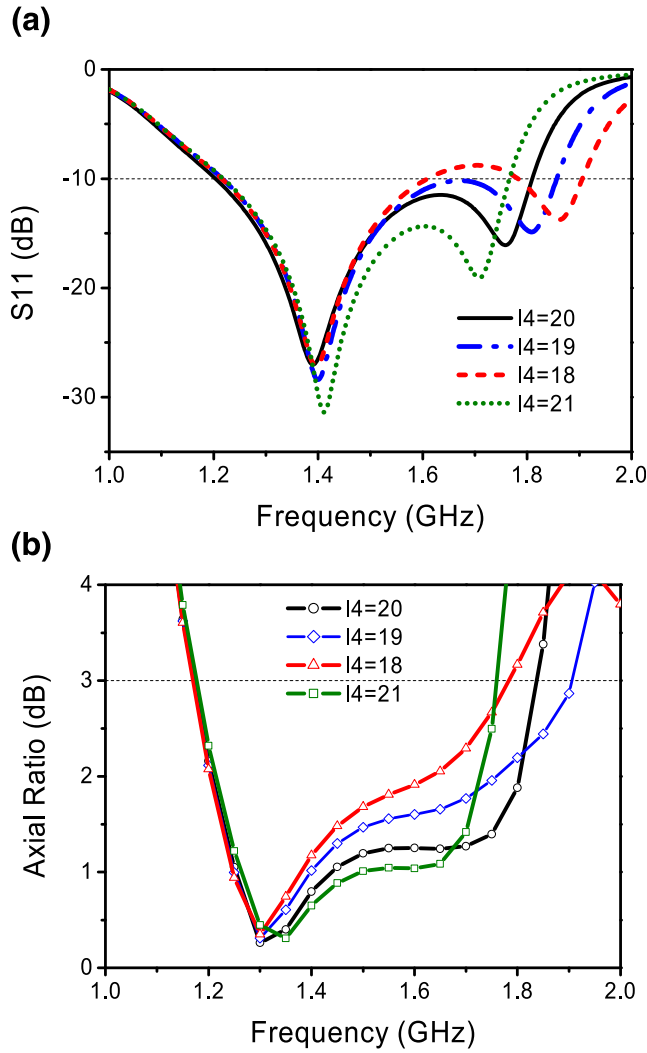**FIGURE 10** Effect of the slot width (s) on (a) S11 (b) Axial ratio

(a)

(b)

FIGURE 11 Effect of vertical resonator length (L$_4$) on (a) S11 (b) Axial ratio

FIGURE 12 Measured S$_{11}$ in comparison with simulation
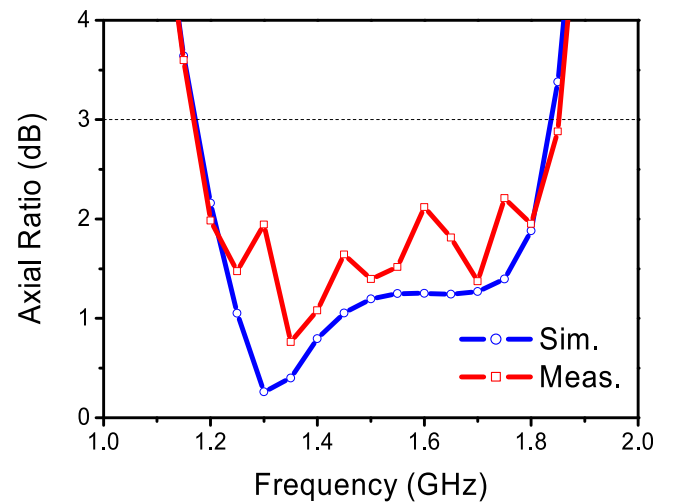
FIGURE 13 Measured axial ratio in comparison with simulation

Q_{ex} are not as accurate and reliable as in the design of conventional microstrip filters. Thus, further extensive parameter study and optimisations were required.

3 | PARAMETRIC STUDY

Couplings among the feedline, the resonator, and the radiation element are complicated by the two signal paths required to excite the vertical and horizontal polarisations from a single feed. Extensive parameter studies and simulations were carried out to optimise both the impedance and the AR bandwidths. Starting from the feedline, Figures 7 and 8 show the effect of the length l_1 and l_2 on impedance matching and AR. As expected, the main impact is on the impedance as these dimensions affect the external coupling (related to Q_{ex}) to the resonator and the L-shaped
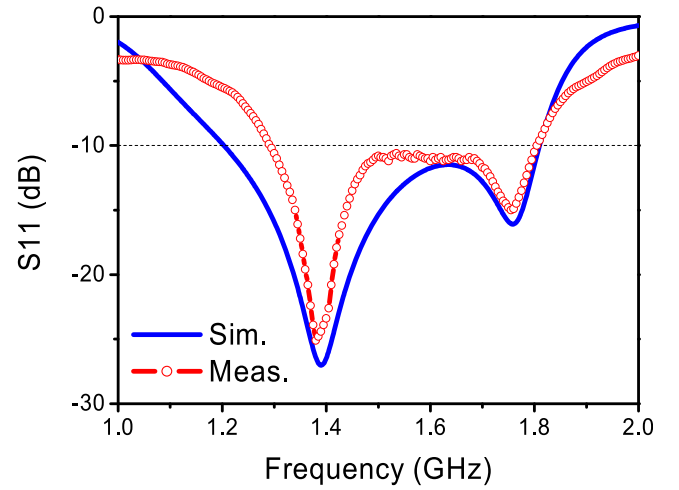
slot. As shown in Figure 7, l_2 plays a key role in broadening the bandwidth. Figure 9 shows the effect of the width of the vertical section of the feedline. This parameter gives another degree of freedom in fine-tuning the impedance matching.

The magnitudes of the horizontal (Ex) and vertical (Ey) electric field must remain nearly the same to control the AR. Retaining those magnitudes can be achieved by controlling the length and width of the L-slot (l_s and s) while monitoring the section lengths of the resonator (l_3, l_4 and l_5). The former alters the dimensions of the vertical and horizontal parts of the radiation aperture, whereas the latter varies the coupling from the resonator to the vertical and horizontal polarisation. The resonator is responsible for feeding the L-slot to excite the two orthogonal modes. By properly placing the resonator behind the L-slot, CP radiation can be realised. Figure 10 shows the important effect

FIGURE 14 Simulated against measured copolarised radiation patterns (a) 1.2 GHz (b) 1.5 GHz (c) 1.8 GHz

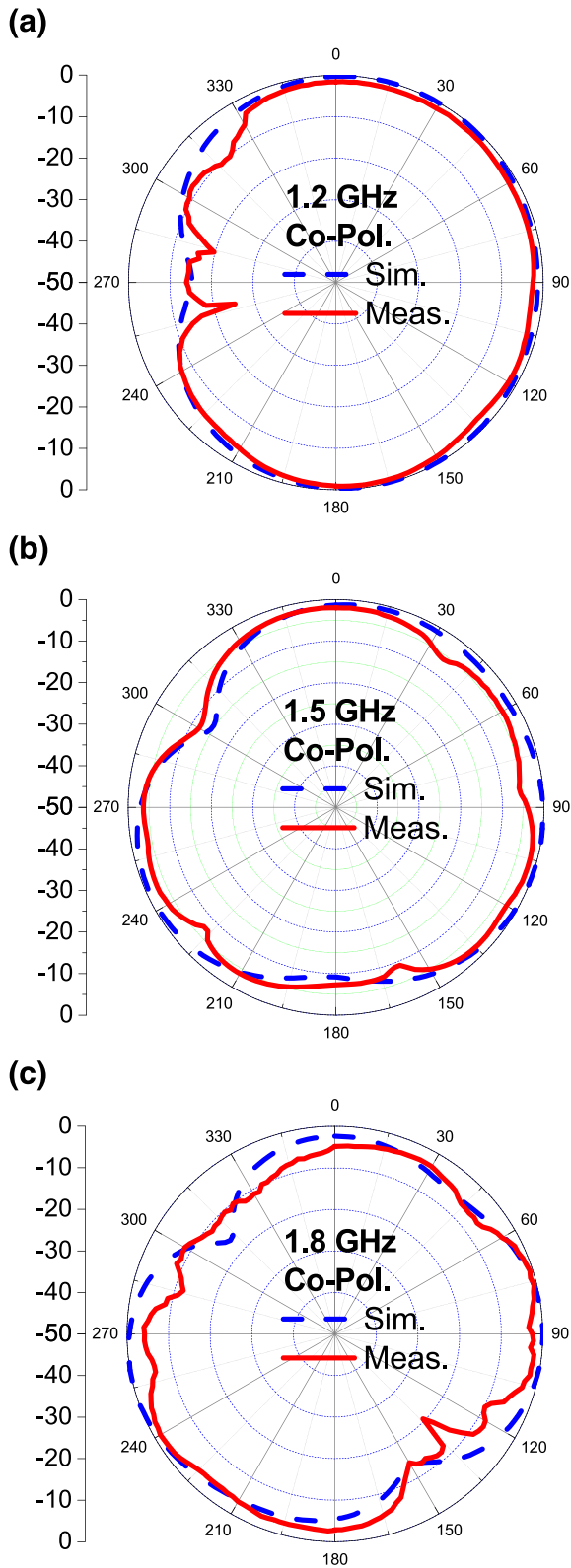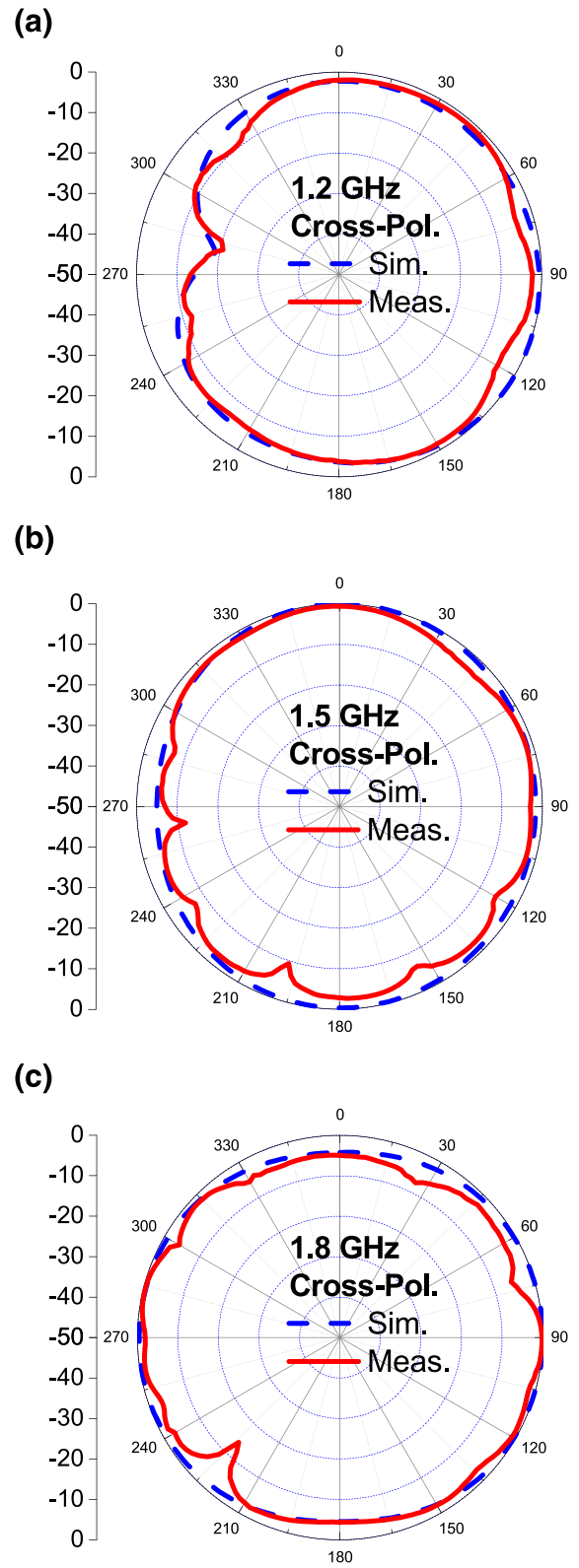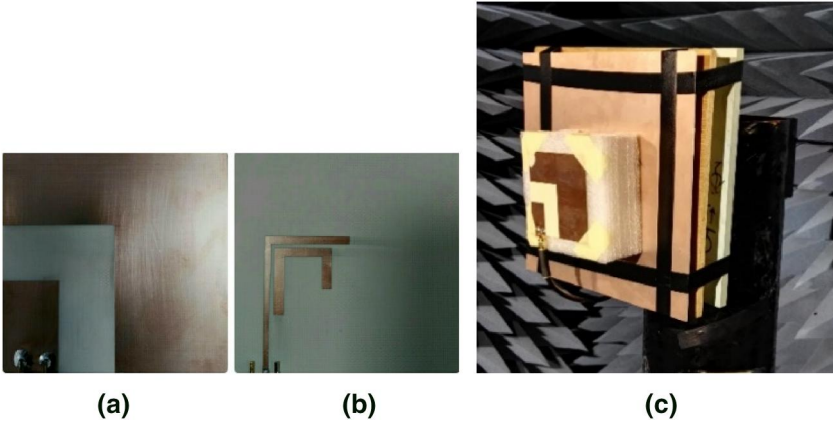**FIGURE 15** Simulated against measured cross-polarised radiation patterns (a) 1.2 GHz (b) 1.5 GHz (c) 1.8 GHz

of the slot width on the AR. It has little to do with the impedance unless it is over 20 mm wide.

Figure 11 shows the effect of varying the vertical length of the resonator (L_4). This parameter clearly tunes the second resonant frequency of the matched antenna and consequently the bandwidth. It is evident that introducing the coupled resonator into the feeding structure contributes to bandwidth control and enhancement. The effects of some parameters (not all are shown) are intertwined, which makes computer-aided optimisation essential but challenging.

4 | SIMULATED AND MEASURED RESULTS

A prototype filter antenna was fabricated and tested. The simulated and measured S_{11} curves are compared in Figure 12. Measurements were conducted using an Agilent Network Analyser N5230 A. A good agreement was achieved with a slightly narrower bandwidth due to the shift of the lower band edge for the measured RLBW to a range of 1.29 to 1.81 GHz (33.5%).

Measured and simulated AR results are compared in Figure 13. Calculations of AR were guided by Equations (4) to (7) [25] using the readings of both the amplitude and the phase from the horizontal and vertical planes (H_A, V_A and H_P, V_p):

$$E_{LHCP} = \frac{1}{\sqrt{2}} \{ [H_A \cos(H_P) + V_A \sin(V_P)] + j[H_A \cos(H_P) - V_A \sin(V_P)] \} \quad (4)$$

$$E_{RHCP} = \frac{1}{\sqrt{2}} \{ [H_A \cos(H_P) - V_A \sin(V_P)] + j[H_A \cos(H_P) + V_A \sin(V_P)] \} \quad (5)$$

$$a.r. = \frac{|E_{RHCP}| + |E_{LHCP}|}{|E_{RHCP}| - |E_{LHCP}|} \quad (6)$$

$$AR = 20 \times \log_{10}(a.r.) \quad (7)$$

Again, a good match between simulation and measurement is obtained at most frequencies. A 46.4% 3 dB ARBW (from 1.16 to 1.86 GHz) is achieved. The entire impedance bandwidth is contained within the ARBW.

Figures 14 and 15 show that the simulated and measured radiation patterns are in broad agreement for co- and cross-polarised cases at the start, centre, and end frequencies of 1.2, 1.5, and 1.8 GHz, respectively. The bidirectional characteristics of the antenna are noticed in the measured radiation patterns. It is worth mentioning that the measurements taken in the range from 180° to 360° may be distorted by the proximity and obstruction of the rotational joint located behind the antenna under test. The configuration of the test setup is not ideal for bidirectional antennas.

5 | INVESTIGATION OF METAL REFLECTOR

The proposed filter antenna is bidirectional, leading to a low average maximum gain of 1.66 dBi across the operation band. The effect of placing a metal reflector of 240×240 mm was investigated. The fabricated filter antenna and a photograph of the prototype inside the anechoic chamber are shown in Figure 16. The reflector was placed behind the substrate at 60 mm (a quarter of a free space wavelength at 1.2 GHz).

The reflection coefficient was not significantly affected by the presence of the reflector, as illustrated in Figure 17 (a) and (b). The AR is degraded in the lower half of the band, as shown in Figure 17(c) and 17(d). The 3 dB ARBW is slightly broadened, however, to 1.13 to 1.9 GHz (50.8%). As shown in Figure 18, the realised gain with the reflector is enhanced, as expected, by more than 3 dBi to a range of 5.5 to 7.2 dBi. A dip can be noted around 1.65 GHz due to the deflected maximum radiation from

(a)

(b)

(c)

(d)
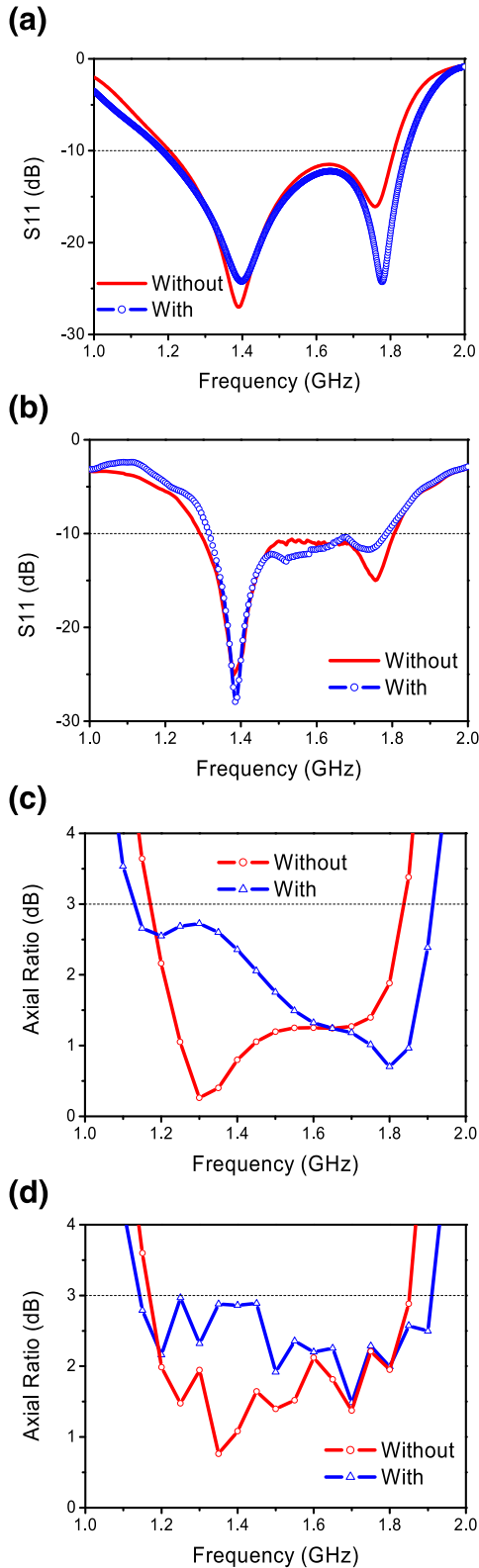
F I G U R E 1 7 Effect of metal reflector: (a) Simulated S11 (b) Measured S11 (c) Simulated axial ratio (d) Measured axial ratio

F I G U R E 1 8 Simulated realised gain with effect of metal reflector
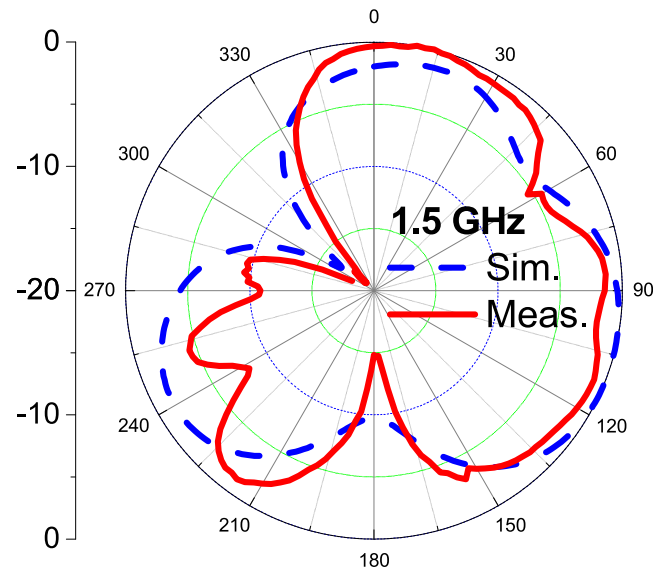
F I G U R E 1 9 Simulated against measured pattern with the reflector at 1.5 GHz

the boresight at that frequency. The measured radiation pattern at the centre frequency of 1.5 GHz is shown in Figure 19. The antenna becomes more directional in the presence of the reflector. This pattern also agrees well with the simulation.

6 | CONCLUSION

A new broadband integrated filtering CP slot antenna was reported. By employing a single resonator coupled to the slot antenna, broad bandwidths for both the RL and the AR were achieved through the mechanism of EM coupling. The coupled-resonator filter approach facilitated the design of the antenna. Broadband RHCP characteristics were obtained without resorting to power dividers or phase shifters. The ARBW contained the entire operational RLBW. Good agreement was achieved between the simulated and measured RL, resulting in a 33.5% (41%) measured (simulated) RLBW.

T A B L E 1 Comparison of circularly polarised antenna performance

Ref.	Ant. Type	Cent. Freq. (GHz)	RLBW (%)	ARBW (%)	Overlapped BW (%)	Gain (dBi)
[3]	Cross-slot	1.565	34	20	58	3.4
[4]	Square patch	2.64	28	10.4	10.4	8.5
[5]	Monopole	2.3	4	4	100	2.7
[11]	Monopole	5.5	149	80.7	52.8	3
[14]	Circular patch	2.5	32.6	33	100	5.2
[15]	L-slot	1.66	30	32	97	2
[19]	Square patch	2.4	8.3	1.35	16.3	3
This work	L-slot	1.55	41	44.5	100	1.7

Abbreviations: Ant., antenna; ARBW, axial ratio bandwidth; BW, bandwidth; Cent. Freq., centre frequency; dBi, decibels-isotropic; RLBW, return loss (over 10 dB) bandwidth.

The measured (simulated) ARBW is 46.4% (44.5%). The bandwidth performance of the proposed antenna is very competitive compared with other CP antennas in the literature. A comparison is presented in Table 1 with the type of antenna, centre frequency, impedance and AR bandwidths, overlapped bandwidth, and finally, the average gain of each design. A good agreement between measured and simulated radiation patterns was also achieved. The effect of placing a metal reflector behind the proposed design was investigated and proven to enhance gain without a significant effect on the RL and AR bandwidths. Because of the integrated resonator, the antenna exhibits a second-order filtering characteristic without cascading a separate filter. This integration approach reduces the complexity and cost of RF front-ends for GNSS applications while controlling bandwidth.

ORCID

Yi Wang https://orcid.org/0000-0002-8726-402X

REFERENCES

1. Gao, S.S., Luo, Q., Zhu, F.: Circularly polarized antennas. John Wiley & Sons, Chichester (2014)
2. Chen, X., et al.: Antennas for global navigation satellite Systems. John Wiley & Sons, Vienna (2012)
3. Aly, M.G., Wang, Y.: A wideband circularly polarised cross-slot antenna with an L- shaped feed-line. In: Loughborough Antennas & Propagation Conference. IET, Loughborough (2017)
4. Chang, F., Wong, K., Chiou, T.-W.: Low-cost broadband circularly polarized patch antenna. IEEE Trans. Antennas Propag. 51(10), 3006–3009 (2003)
5. Ghobadi, A., Dehmollaian, M.: A printed circularly polarized Y-shaped monopole antenna. Antennas Wirel. Propag. Lett. 11, 22–25 (2012)
6. Song, C., et al.: A broadband circularly polarized cross-dipole antenna for GNSS applications. In: Loughborough Antennas & Propagation Conference. IEEE, Loughborough (2015)
7. Nosrati, M., Tavassolian, N.: Miniaturized circularly polarized square slot antenna with enhanced axial-ratio bandwidth using an antipodal Y-strip. IEEE Antennas Wirel. Propag. Lett. PP(99), 1–4 (2016)
8. Pan, S.P., Sze, J.Y., Tu, P.J.: Circularly polarized square slot antenna with a largely enhanced axial-ratio bandwidth. IEEE Antennas Wirel. Propag. Lett. 11, 969–972 (2012)
9. Tang, H., et al.: Compact broadband CP monopole antenna with tilted branch. Electron Lett 52(21), 1739–1740 (2016)
10. Ding, K., et al.: Broadband C-shaped circularly polarized monopole antenna. IEEE Trans. Antennas Propagat. 63(2), 785–790 (2015)
11. Cahndu, D., Karthikeyan, S.S.: A novel broadband dual circularly polarized microstrip-fed monopole antenna. IEEE Trans. Antennas Propag. 65(3), 1410–1415 (2017)
12. Lertsakwimarn, K., Phongcharoenpanich, C., Fukusako, T.: A ring antenna for dual-sense circular polarization. In: IEEE International Conference on Computational Electromagnetics, pp. 194–196. IEEE, Guangzhou (2016)
13. Chen, J.-M., Row, J.-S.: Wideband circularly polarized slotted-patch antenna with a reflector. Antennas Wirel. Propag. Lett. 14, 575–578 (2015)
14. Zhu, W., et al.: Broadband and dual circularly polarized patch antenna with H-shaped aperture. In: 2014 International Symposium on Antennas and Propagation Conference Proceedings, pp. 549–550. IEEE, Kaohsiung (2014)
15. Mousavi, P., Miners, B., Basir, O.: Wideband L-shaped circular polarized monopole slot antenna. Antennas Wirel. Propag. Lett. 9, 822–825 (2010)
16. Mao, C.-X., et al.: Multimode resonator-fed dual-polarized antenna array with enhanced bandwidth and selectivity. IEEE Trans. Antennas Propagat. 63(12), 5492–5499 (2015)
17. Ogbodo, E.A., et al.: Dual-band filtering antenna using dual-mode patch resonators. Microw Opt Technol Lett 60(10), 2564–2569 (2018)
18. Cheng, W., Li, D.: Circularly polarised filtering monopole antenna based on miniaturised coupled filter. Electron Lett. 53(11), 700–702 (2017)
19. Bao, X., et al.: Differentially-fed omnidirectional circularly polarized patch antenna for RF energy harvesting.In: 10th European Conference on Antennas and Propagation, pp. 1–5 (2016)
20. Wu, W., et al.: Design of A Compact fitler-antenna using DGS structure for modern wireless communication Systems. In: 2013 5th IEEE International Symposium on Microwave, Antenna, Propagation and EMC Technologies for Wireless Communications, 355–358 (2013)

21. Wu, W., et al.: A broadband low profile microstrip filter-antenna with an omni-directional pattern. In: Proceedings of 2014 3rd Asia-Pacific Conference on Antennas and Propagation, pp. 580–582. IEEE, Harbin (2014)

22. Zhang, X.Y., Duan, W., Pan, Y.-M.: High-gain filtering patch antenna without extra circuit. IEEE Trans. Antennas Propagat. 63(12), 5883–5888 (2015)

23. Balanis, C.A.: Antenna Theory Analysis and Design, vol. 28(3), 3rd ed. John Wiley & Sons, Toronto (2012)

24. Hong, J., Lancaster, M.J.: Microstrip Filters for RF/Microwave Applications, vol. 7. John Wiley & Sons, New York (2001)

25. Toh, B.Y., Cahill, R., Fusco, V.F.: Understanding and measuring circular polarization. IEEE Trans Educ. 46(3), 313–318 (2003)